3rd EUROPEAN CONFERENCE ON
EARTHQUAKE ENGINEERING & SEISMOLOGY
BUCHAREST, ROMANIA, 2022

# Tangent-stiffness-proportional viscous damping independent of the geometric stiffness matrix.

**Jose Fernando Baena-Urrea** – Ph.D. student, Institute of Mechanics, Materials and Civil Engineering, UCLouvain, Belgium, jose.baenaurrea@uclouvain.be

**João Pacheco de Almeida** – Assistant Professor, Institute of Mechanics, Materials and Civil Engineering, UCLouvain, Belgium, joao.almeida@uclouvain.be

**Abstract:** This paper presents a tangent-stiffness-proportional viscous damping model independent of the geometric stiffness for time-history response simulation of frame structures. The nonlinear geometric effects are considered using a corotational formulation that allows to isolate the nonlinear effects of material and geometric sources, as well as the corresponding tangent stiffness contributions. Therefore, non-directly modelled sources of energy dissipation can be made proportional just to the material stiffness matrix term. After presenting the formulation and discussing the physical significance of the proposed model, an illustrative example of a slender reinforced concrete column is presented. Comparisons with the widely used total-tangent-stiffness-proportional approach show the advantages of the current proposal.

**Keywords:** corotational formulation, time-history analysis, rayleigh damping, geometric stiffness matrix

## 1. Introduction

The use of nonlinear analyses has spread during the last decades among the engineering community due to the availability of more advanced models and software running on increasingly powerful hardware, as well as the growing relevance of performance-based design and assessment of structures (Golesorkhi et al. 2017). Limit states associated with severe damage and collapse can be reached when structures are subjected to extreme loads, where nonlinear geometric effects often play an important role (Hardyniec and Charney 2015).

For extreme loads and systems susceptible to large deformations, neglecting nonlinear geometric effects in the numerical response of the structure can lead to erroneous and unconservative analyses. However, the inclusion of these effects can also bring unwarranted consequences when considered in the definition of viscous Rayleigh damping (RD). This model is widely used as a proxy to simulate the energy dissipation of several complex mechanisms in structures, such as micro hysteretic curves of materials in the elastic range, friction between structural and nonstructural components, among others (Leger and Dussault 1992; Kareem and Gurley 1996).

The system of equations expressing the dynamic equilibrium of a nonlinear multi-degree-of-freedom (MDoF) planar (2D) system with viscous damping is as follows:

$$\begin{bmatrix} \boldsymbol{M}_{tt} & 0 \\ 0 & 0 \end{bmatrix} \begin{Bmatrix} \ddot{\boldsymbol{U}}_t(t) \\ \ddot{\boldsymbol{U}}_0(t) \end{Bmatrix} + \begin{bmatrix} \boldsymbol{C}_{tt} & \boldsymbol{C}_{t0} \\ \boldsymbol{C}_{0t} & \boldsymbol{C}_{00} \end{bmatrix} \begin{Bmatrix} \dot{\boldsymbol{U}}_t(t) \\ \dot{\boldsymbol{U}}_0(t) \end{Bmatrix} + \{\boldsymbol{f}(\boldsymbol{U}(t))\} = \begin{Bmatrix} -\boldsymbol{M}_{tt}\boldsymbol{J}_x\ddot{u}_{gx}(t) \\ 0 \end{Bmatrix} + \begin{Bmatrix} \boldsymbol{P}_{gt} \\ \boldsymbol{P}_{g0} \end{Bmatrix} \quad (1)$$

where $\boldsymbol{M}$ and $\boldsymbol{C}$ are the mass and damping matrices, respectively, and $\{\boldsymbol{f}(\boldsymbol{U}(t))\}$ expresses the nonlinear relation between resisting forces and displacements. The

subscripts *t* and *0* refer to degrees of freedoms (DoFs) with and without mass. The vectors $\boldsymbol{U}$ , $\dot{\boldsymbol{U}}$, and $\ddot{\boldsymbol{U}}$ depict the relative displacement, velocity, and acceleration of the DoFs. The right-hand of the equation contains two loading vectors corresponding to a time-varying component and a constant term. The former represents the effective earthquake forces where $\boldsymbol{J}_x$ is the influence vector and $\ddot{u}_{gx}(t)$ is the corresponding component of the ground motion record. The gravity or static forces $\begin{Bmatrix}\boldsymbol{P}_{gt}\\ \boldsymbol{P}_{g0}\end{Bmatrix}$ can be applied in all the DoFs of the structure.

Using RD, the damping matrix $\boldsymbol{C}$ is obtained, with eq. (2), as a linear combination of the mass and stiffness ($\boldsymbol{K}$) matrices. The multiplication coefficients are found from specified input damping ratios at two distinct frequencies with eq. (3) (Chopra 2015). This method, inherited from linear analysis, has shortcomings and inconsistencies when implemented for nonlinear response simulation, as recalled in more detail in this section. One of these inconsistencies, studied in the present work, is the physically groundless presence of the geometric stiffness matrix contribution (GSM) in the definition of the stiffness-proportional term of the damping matrix, which appears when nonlinear geometric effects are considered.

$$\begin{bmatrix}\boldsymbol{C}_{tt} & \boldsymbol{C}_{t0}\\ \boldsymbol{C}_{0t} & \boldsymbol{C}_{00}\end{bmatrix} = a_0\begin{bmatrix}\boldsymbol{M}_{tt} & 0\\ 0 & 0\end{bmatrix} + a_1\begin{bmatrix}\boldsymbol{K}_{tt} & \boldsymbol{K}_{t0}\\ \boldsymbol{K}_{0t} & \boldsymbol{K}_{00}\end{bmatrix} \tag{2}$$

$$\begin{Bmatrix}\zeta_i\\ \zeta_j\end{Bmatrix} = \frac{1}{2}\begin{bmatrix}\omega_i^{-1} & \omega_i\\ \omega_j^{-1} & \omega_j\end{bmatrix}\begin{Bmatrix}a_0\\ a_1\end{Bmatrix} \tag{3}$$

The numerical simplicity of this model has made RD ubiquitous in FE software and the most common model for viscous damping in nonlinear dynamic analyses. In the case of a building, the mass-proportional term is difficult to interpret from the physical viewpoint because it would correspond to damping caused by the medium surrounding the structure or by the sliding masses, while the stiffness-proportional term is usually more straightforwarly understood as proportional to the deformations between floors.

The mass-proportional term has been criticized because it can lead to unconservative results in nonlinear analyses, resulting in high damping forces compared to restoring forces (Hall 2006; Erduran 2012). In base-isolated systems, this arises in the overall structure when the damping matrix is defined based on the properties of the stiffer structure, resulting in a high effective damping ratio imparted by the mass-proportional damping term. The initial stiffness-proportional damping model leads to unrealistic response for yielding systems (Correia et al. 2013), creation of high spurious resisting damping forces, and moments in the massless DoFs (Bernal 1994). The latter moments can reach the yielding capacity of the structural elements and cause a general increase in the effective damping ratio of the structure, as indicated by Chrisp (1980), Bernal (1994), and Charney (2008).

To reduce the spurious damping forces caused by the stiffness-proportional term of RD, several authors (Leger and Dussault 1992; Charney 2008; Petrini et al. 2008; Sousa et al. 2020) proposed updating the damping matrix with the tangent stiffness. It is now widely accepted that using the latter choice as damping proportionality matrix provides more physically meaningful results than the initial stiffness matrix (Priestley and Grant 2005; Chambreuil et al. 2021). In fact, the nonlinear relations $\{\boldsymbol{f}(\boldsymbol{U}(t))\}$ in eq. (1) are expected to simulate most of the energy dissipation through hysteretic response as displacement demands increase and yielding mechanisms gradually develop, implying that the

contribution of the damping model for energy dissipation should consequently be reduced. Since the tangent stiffness matrix reflects the course of such yielding, its choice is therefore compelling. This consideration is adopted in the present paper and refined in the next section. Other related problems are widely discussed in the literature, such as the significant decrease in the effective structural damping ratio when the stiffness decreases, as reported by Charney (2008) and Leger and Dussault (1992). To address this issue, the latter researchers proposed to update at each step the damping parameters $a_0$ and $a_1$ with the frequencies found using the tangent stiffness.

Even though using the tangent stiffness partially solves some of the challenges of RD, it is not recommended by other researchers like Chopra and Mckenna (2016) who argue that the model has several conceptual limitations and a high calculation cost when the damping parameters are updated. The computation of the damping matrix at each step using the tangent stiffness matrix results in damping force-velocity relationships that exhibit hysteresis. In addition, for large deformations, negative damping forces can appear due to the negative slope in hysteretic nonlinear material rules or the effect of the GSM.

The purpose of this study is to propose and investigate a redefinition of the stiffness-proportional term of RD that excludes the contribution of the GSM, which has been included in all previous versions of this widely used damping model. Section 2 explains briefly the theoretical background of the new model whereas Section 3 presents an illustrative slender reinforced concrete column studied in detail, highlighting the innovative aspects and advantages of the current proposal. The conclusions and the outlook of this work are presented in the last section.

## 2. Material-tangent-stiffness-proportional damping model (MTSPD)

### 2.1. Material and geometric terms of the stiffness matrix using a corotational formulation

The corotational approach expresses the beam elemental displacements and internal forces in the three reference systems shown in Fig. 1 for a planar case: global (gl), local (loc), and basic (bsc). The basic system is defined with the current position of the element's nodes and follows the element as it deforms, allowing for a separation between the rigid body motion and the internal deformations. The latter are expressed in eq. (4), at the basic reference system, in terms of the local displacements ($\boldsymbol{u}^{loc}$) and the corotating angle ($\beta$) between the local and the basic reference system.

$$u_1^{bsc} = l(\boldsymbol{u}^{loc}) - l_0, \qquad u_2^{bsc} = u_3^{loc} - \beta, \qquad u_3^{bsc} = u_6^{loc} - \beta \qquad (4)$$

where $l(\boldsymbol{u}^{loc})$ and $l_0$ are the current deformed length and the undeformed length of the element, respectively.

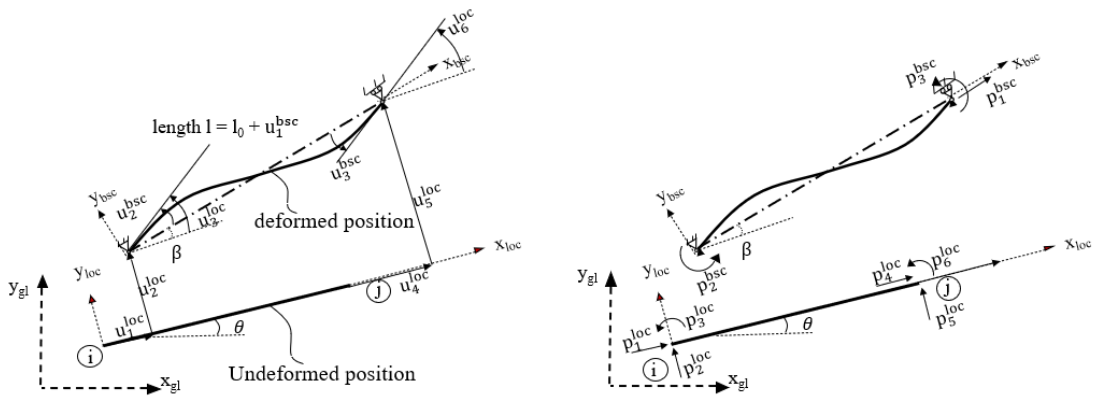


Fig. 1 - Element forces and displacements expressed in the different reference systems**.**

The incremental compatibility ($\boldsymbol{\Gamma_C}(\boldsymbol{u}^{loc})$) matrix is obtained by differenting $\frac{\partial \boldsymbol{u}^{bsc}}{\partial \boldsymbol{u}^{loc}}$. At the basic level, it is possible to obtain the constitutive relations expressing the basic forces as a function of the basic displacements ($\boldsymbol{p}^{bsc}(\boldsymbol{u}^{bsc})$). After they are found, they can be expressed in the local reference system ($\boldsymbol{p}^{loc}$) using equilibrium relations derived by equilibrium in the deformed configuration.

$$\boldsymbol{p}^{loc} = \boldsymbol{\Gamma}_E(\boldsymbol{u}^{loc}) \cdot \boldsymbol{p}^{bsc}(\boldsymbol{u}^{bsc}) = \left(\boldsymbol{\Gamma}_C(\boldsymbol{u}^{loc})\right)^T \cdot \boldsymbol{p}^{bsc}(\boldsymbol{u}^{bsc}) \qquad (5)$$

The incremental relation between the global structural forces and displacements is required to solve the nonlinear problem and define a tangent-stiffness-proportional damping (TSPD). At the local reference system, the tangent elemental stiffness ($\boldsymbol{k}^{TanLoc}$) is found through differentiation of eq. (5) with respect to the local displacements:

$$\boldsymbol{k}^{TanLoc} = \frac{\partial \boldsymbol{p}^{loc}}{\partial \boldsymbol{u}^{loc}} = \underbrace{\frac{\partial (\boldsymbol{\Gamma}_E(\boldsymbol{u}^{loc}))}{\partial \boldsymbol{u}^{loc}} \cdot \boldsymbol{p}^{bsc}}_{\boldsymbol{k}^{TanGeoLoc}} + \underbrace{\boldsymbol{\Gamma}_c(\boldsymbol{u}^{loc})^T \cdot \frac{\partial (\boldsymbol{p}^{bsc}(\boldsymbol{u}^{bsc}))}{\partial \boldsymbol{u}^{bsc}} \cdot \boldsymbol{\Gamma}_C(\boldsymbol{u}^{loc})}_{\boldsymbol{k}^{TanMatLoc}} \qquad (6)$$

The application of the chain rule of differentiation to the second term on the right-hand side brings out the incremental relation between the basic forces and the basic displacements, which is obtained according to the element formulation. The first and second terms on the right side of the equation above are the geometric and material components of the elemental stiffness matrix, respectively. The elemental global forces, and tangent stiffness matrix are then found with a rotation matrix considering the angle (θ) between the global and the local reference systems, and assembled to obtain the global resisting forces and tangent stiffness of the structure.

## 2.2. Motivation and formulation

As discussed, the most accepted models for RD or stiffness-proportional damping (SPD) models have previously been defined as proportional to the total tangent stiffness matrix (TSM) $\boldsymbol{K}^{Tan}$. The total stiffness matrix also determines the natural frequencies of the structure, which in turn are typically used to estimate the damping parameters $a_0$ and $a_1$ (for RD) or just $a_1$ (for SPD).

The present proposal uses a corotational formulation that allows a decomposition of the total tangent stiffness matrix of the structure into a material tangent stiffness matrix $\boldsymbol{K}^{TanMat}$ and a geometric tangent stiffness matrix $\boldsymbol{K}^{TanGeo}$, denoted with the acronyms MSM and GSM, respectively. The advantages of using the above decomposition are that

it allows the MSM to be defined as a proportionality matrix for the damping model using consequential damping parameters $a_0$ and $a_1$ determined using the natural frequencies found with MSM alone. As far as the authors are aware, only Charney (2008) has briefly suggested not including the GSM in the calculation of the stiffness-proportional term of Rayleigh-based damping models.

This approach aims at anchoring energy-dissipation simulation to material-related mechanisms. The extended physical meaningfulness of the material tangent stiffness proportional damping (MTSPD) herein proposed and studied preserves the advantages of SPD. Moreover, the new MTSPD avoids the introduction of energy into the post-peak response of MDoF systems due to nonlinear geometric effects that can occur when simulating the response of flexible structures under extreme loading events.

Eq. (7) gives the damping matrix using the proposed damping model:

$$\begin{bmatrix} \boldsymbol{C}_{tt}^{Mat} & \boldsymbol{C}_{t0}^{Mat} \\ \boldsymbol{C}_{0t}^{Mat} & \boldsymbol{C}_{00}^{Mat} \end{bmatrix} = a_{1M} \begin{bmatrix} \boldsymbol{K}_{tt}^{TanMat} & \boldsymbol{K}_{t0}^{TanMat} \\ \boldsymbol{K}_{0t}^{TanMat} & \boldsymbol{K}_{00}^{TanMat} \end{bmatrix} \tag{7}$$

The damping parameter can be defined using the desired frequency according to following expression:

$$a_1 = \frac{2\zeta_i}{\omega_i} \tag{8}$$

The damping parameter $a_1$ is commonly defined using the first mode's frequency satisfying eq. (9), in which case it is denoted $a_{1T}$. In this work, the damping parameter $a_1$ is defined with the first mode's frequency satisfying eq. (10) and denoted $a_{1M}$.

$$\boldsymbol{K}^{Tan}\boldsymbol{\phi}_1 = \omega_T^2 \boldsymbol{M}\boldsymbol{\phi}_1 \tag{9}$$

$$\boldsymbol{K}^{TanMat}\boldsymbol{\phi}_1 = \omega_M^2 \boldsymbol{M}\boldsymbol{\phi}_1 \tag{10}$$

where $\boldsymbol{K}^{Tan}$ and $\boldsymbol{K}^{TanMat}$ in eqs. (7), (9), and (10) are the total tangent stiffness matrix TSM and material tangent stiffness matrix MSM at the first step after applying the axial loads. $\omega_T$, $\omega_M$, and $\boldsymbol{\phi}_1$ are the frequencies and modal shapes satisfying eqs. (9) and (10). The models investigated and compared in the current work are summarised in Table 1.

*Table 1. Tangent-stiffness-proportional damping models analysed.*

| Complete name | Damping parameter | Nomenclature | Expression |
|---|---|---|---|
| Total tangent stiffness-proportional viscous damping model | $a_{1T}$ | TTSPD_$a_{1T}$ | $\boldsymbol{C} = a_{1T}\,\boldsymbol{K}^{Tan}$ |
| Material tangent stiffness-proportional viscous damping model | $a_{1M}$ | MTSPD_$a_{1M}$ | $\boldsymbol{C}^{Mat} = a_{1M}\,\boldsymbol{K}^{TanMat}$ |

## 3. Numerical cases studies

Fig. 2 presents the structure that is used to illustrate the advantages and specificities of the proposed MTSPD model. As recalled in the previous section, the influence of the GSM becomes important in slender structures subjected to significant axial loads. Consider a cantilever column represented in Fig. 2 (a), which is subdivided into two force-based elements (Calabrese et al. 2010) using the cross-section presented and discretised in Fig. 2 (b) and the material rules of Table 2. The steel fibres employ the model by Menegotto and Pinto (1973) and the 64 concrete fibres along the height of the section use the model of Mander et al. (1988). The reinforced concrete column has a

translational mass ($M_{translation} = 10$ ton) and rotational inertia ($M_{rotation} = 1.0$ ton $\cdot$ $m^2$ ) at the top. At the first step, an axial load is imposed to the system to apply a specific axial load ratio (ALR).

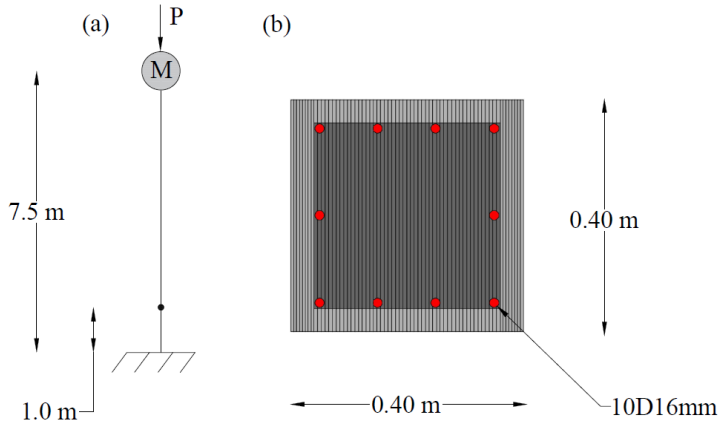


Fig. 2 - (a) Cantilever reinforced concrete column modelled with two corotational force-based elements. (b) Fibre cross-section of the column.

*Table 2. Material parameters of the models used for steel and concrete fibres.*

| **Steel Fibres** | **$f_y$ (MPa)** | **$E_o$ (GPa)** | **b** | **R0** | **$A_1$** | **$A_2$** | **$A_3$** | **$A_4$** |
|---|---|---|---|---|---|---|---|---|
| Steel bars | 515 | 210 | 0.00 | 20.00 | 19.25 | 0.15 | 0.00 | 1.00 |
| **Concrete Fibres** | **$f_c$ (MPa)** | **$E_o$ (GPa)** | **$\varepsilon_{cu}$** | **$f_t$ (MPa)** | **$\varepsilon_t$** | **beta** | | |
| Concrete cover | 28.0 | 24.9 | 0.004 | 0 | 0 | 0.1 | | |
| Concrete core of the sections in the element at the base | 41.7 | 35.4 | 0.020 | 0 | 0 | 0.1 | | |
| Concrete core of the sections in the element at the top | 32.2 | 28.6 | 0.016 | 0 | 0 | 0.1 | | |

The GSM affects the computed natural frequency ($\omega_T$) of the system and thus the damping parameters ($a_T$). This effect may not be negligible for slender structures where the contribution of the GSM to the TSM is significant. This effect can be observed in Fig. 3, which shows the variation of the fundamental frequency of the column under varying ALR. The fundamental frequency approaches a null value near the critical buckling load, and increases for less compressive values of the ALR. Conversely, the natural frequency independent of the GSM ($\omega_M$) does not present significant changes under compressive ALRs. Such small variation is only due to the reduction in the concrete Young modulus as the compressive load increases. Under positive ALR the stiffness of the concrete fibres is equal to zero, and the stiffness comes solely from the steel rebars. Thus, the fundamental frequency changes considerably when the concrete section is cracked.

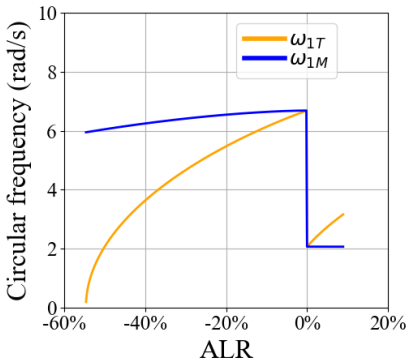


Fig. 3 - Influence of the ALR (negative: compression) on the first natural frequency of the RC column.

The variation of the fundamental horizontal frequency will also affect the damping parameter $a_1$. Fig. 4 shows that the damping parameter $a_{1T}$ increases sharply for highly-compressive ALR. Additionally, there is an opposite less critical effect under increasing ALR in tension, steadily reducing the magnitude of the damping parameter. The latter effects are not present in the damping parameter $a_{1M}$, which is independent of the GSM and depends only on material-related mechanisms.

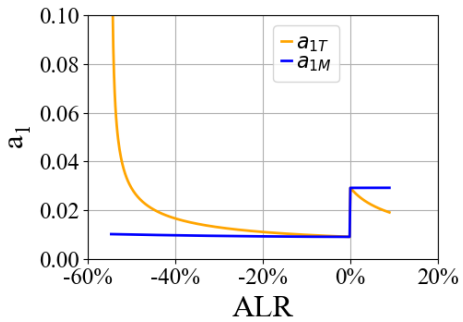


Fig. 4 - Evolution of the damping parameter $a_1$ for damping ratio of 2% at the first natural frequency.

After imposing the specific ALR, the cantilever is subjected to the horizontal component of the Loma Prieta earthquake downloaded from the strong motion database of the Pacific Earthquake Engineering Research Center (2005) and shown in Fig. 5 (1989, $M_w$=6.2, station: APEEL 10 – Skyline). The traditional TTSPD_$a_{1T}$ approach and the MTSPD_ $a_{1M}$ model are compared assuming a damping ratio of 2% associated with the fundamental frequency, which is a commonly accepted value for nonlinear time-history analysis of reinforced concrete structures without non-structural elements.

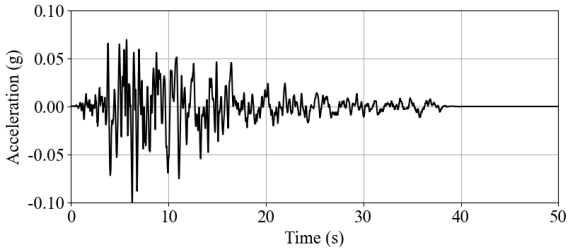


Fig. 5 - Ground motion record from the Loma Prieta earthquake (1989).

The lateral displacement response at the top of the column with two different ALR and both damping models is shown in Fig. 6. It can be observed that the TTSPD_$a_{1T}$ outputs higher displacements and a slower movement decay at the last part of the response, which indicates a smaller effective damping ratio compared to the model MTSPD_$a_{1M}$. It is also apparent that the difference between both models increases for more compressive ALR, since the relative importance of GSM becomes higher in comparison to the MSM. Additionally, the time-history response of bending moment and curvature of the cross-

section at the base of the column, presented in Fig. 7 and Fig. 8, also exhibit significant differences that increase for higher compressive loads.

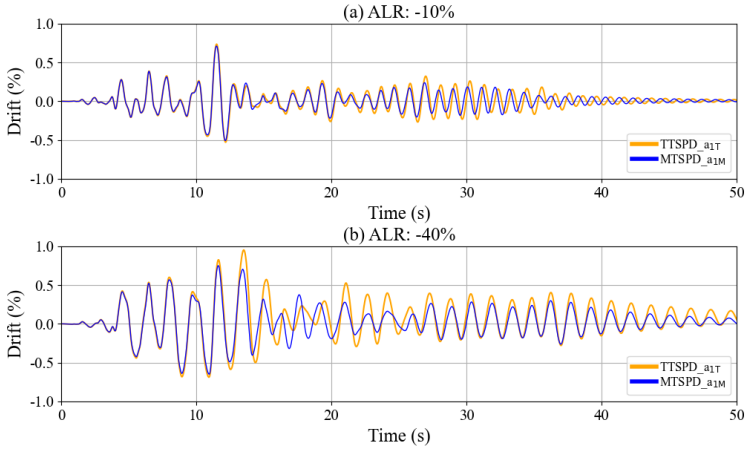


Fig. 6 - Time-history response of cantilever top horizontal displacement under different compressive ALRs, for models MTSPD_$a_{1M}$ and TTSPD_$a_{1T}$.

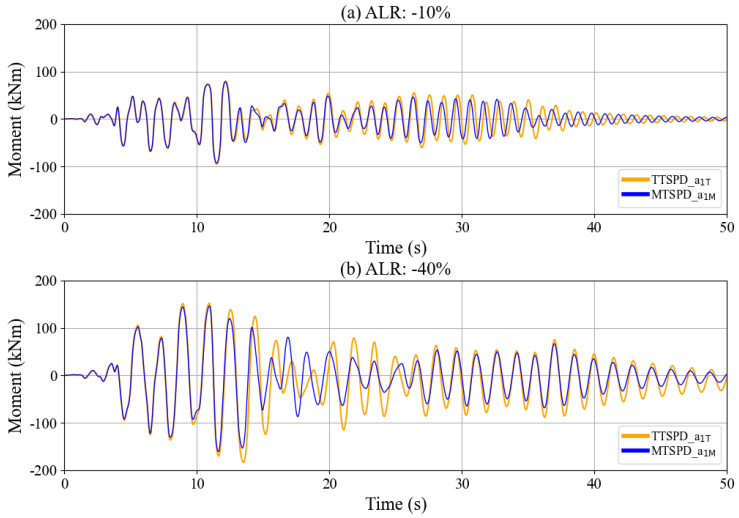


Fig. 7 - Time-history of base cross-section bending moment under different compressive ALRs, for models MTSPD_$a_{1M}$ and TTSPD_$a_{1T}$.

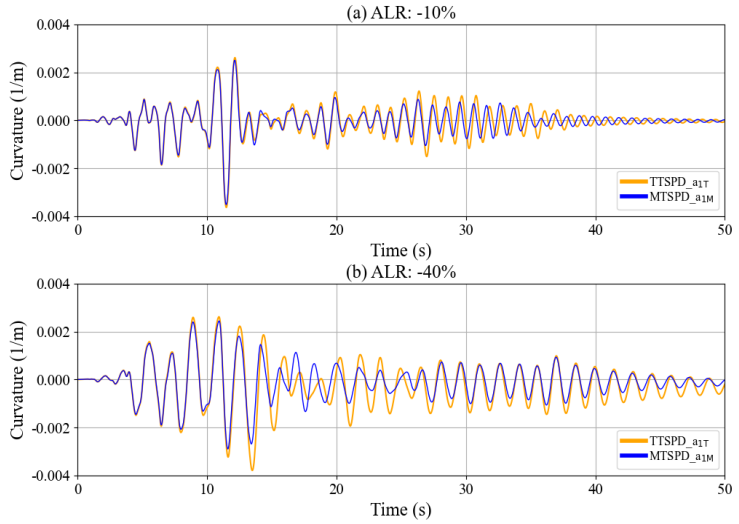


Fig. 8 - Curvature of the cross-section at the base under different compressive ALRs, for models MTSPD_$a_{1M}$ and TTSPD_$a_{1T}$.

This study case illustrates the practical influence of the GSM on the definition of the damping model, both as a proportionality matrix and through the calculation of the damping parameter. The response of the structure is different in terms of global displacements, internal forces, and deformations, even for small ALRs, increasing significantly for higher compressive loads. Typically, the damage index of structural elements depends on the reached maximal deformation response and/or the hysteretic rules' total energy (Park et al. 1987), and consequently the definition of a damping matrix including or excluding the GSM will also affect the assessment of the structure.

## 4. Conclusions

This paper briefly presents a new viscous damping model solely proportional to the tangent material stiffness matrix (MSM), i.e. independent of the tangent geometric stiffness matrix (GSM). Its application to a slender reinforced concrete column, followed by a nonlinear dynamic analysis, reveals that the GSM affects the definition of non-directly modelled sources of energy dissipation and the overall structural response. The traditional total-tangent-stiffness proportional damping (TTSPD_$a_{1T}$) can be significantly affected by the GSM, which however reflects no clearly established link with energy-dissipation mechanisms. The magnitude of the damping matrix changes considerably as a function of the external axial load applied on the member.
This investigation proposes a more physically consequential choice for the definition of tangent-stiffness-proportional damping models, based on adopting a matrix proportional to the MSM and a damping parameter computed from the natural frequency found with the MSM alone.

### Acknowledgements

The authors want to express their gratitude to the Fonds Speciaux de Recherche of the Université catholique de Louvain (UCLouvain) for funding this research through the Grants FSR 2018 and FSR 2021.

## 5. References

Bernal D (1994) Viscous damping in inelastic structural response. Journal of Structural Engineering 120:1240–1254

Calabrese A, Almeida JP, Pinho R (2010) Numerical issues in distributed inelasticity modeling of RC frame elements for seismic analysis. Journal of Earthquake Engineering 14:38–68. https://doi.org/10.1080/13632461003651869

Chambreuil C, Giry C, Ragueneau F, Léger P (2021) Seismic energy dissipation in reinforced concrete beam: investigating damping formulations. European Journal of Environmental and Civil Engineering 1–27. https://doi.org/10.1080/19648189.2021.2009380

Charney FA (2008) Unintended Consequences of Modeling Damping in Structures. Journal of Structural Engineering 134(4):581–592. https://doi.org/10.1061/ASCE0733-94452008134:4581

Chopra AK (2015) Dynamics of structures theory and applications to earthquake engineering, Fourth edition. Prentice Hall, Boston, USA

Chopra AK, Mckenna F (2016) Modeling viscous damping in nonlinear response history analysis of buildings for earthquake excitation. Earthquake Engineering and Structural Dynamics 45:193–211

Chrisp D (1980) Damping models for inelastic structures. Master's Thesis, University of Canterbury, Christchurch, New Zealand

Correia A, Almeida JP, Pinho R (2013) Seismic energy dissipation in inelastic frames: Understanding state-of-the-practice damping models. Structural Engineering International: Journal of the International Association for Bridge and Structural Engineering (IABSE) 23:148–158. https://doi.org/10.2749/101686613X13439149157001

Erduran E (2012) Evaluation of Rayleigh damping and its influence on engineering demand parameter estimates. Earthquake Engineering and Structural Dynamics 41:1905–1919. https://doi.org/10.1002/eqe.2164

Golesorkhi R, Joseph LM, Klemencic R, et al (2017) Performance-based seismic design for tall buildings : an output of the CTBUH Performance-Based Seismic Design Working Group. CTBUH Headquarters, Chicago, USA

Hall JF (2006) Problems encountered from the use (or misuse) of Rayleigh damping. Earthquake Engineering and Structural Dynamics 35:525–545

Hardyniec A, Charney F (2015) An investigation into the effects of damping and nonlinear geometry models in earthquake engineering analysis. Earthquake Engineering and Structural Dynamics 44:2695–2715. https://doi.org/10.1002/eqe.2604

Kareem A, Gurley K (1996) Damping in structures: Its evaluation and treatment of uncertainty. Journal of Wind Engineering and Industrial Aerodynamics 59:131–157. https://doi.org/10.1016/0167-6105(96)00004-9

Leger P, Dussault S (1992) Seismic-energy dissipation in MDOF structures. Journal of Structural Engineering 118(5):1251–1269

Mander JB, Priestley MJN, Park R (1988) Theoretical stress-strain model for confined concrete. Journal of Structural Engineering 114:1804

Menegotto M, Pinto PE (1973) Method of analysis for cyclically loaded r.c. plane frames including changes in geometry and non-elastic behaviour of elements under combined normal force and bending. IABSE reports of the working commissions 13:15–22. https://doi.org/10.5169/seals-13741

Pacific Earthquake Engineering Research Center. (2005) PEER Strong Motion Database on Line. In: https://peer.berkeley.edu/peer-strong-ground-motion-databases

Park Y, Ang A, Wen Y, Eeri M (1987) Damage-limiting aseismic design of buildings. Earthquake spectra 3:1–26

Petrini L, Maggi C, Priestley N, Calvi G (2008) Experimental verification of viscous damping modeling for inelastic time history analyzes. Journal of Earthquake Engineering 12:125–145. https://doi.org/10.1080/13632460801925822

Priestley MJN, Grant DN (2005) Viscous damping in seismic design and analysis. Journal of Earthquake Engineering 9:229–255

Sousa R, Almeida JP, Correia AA, Pinho R (2020) Shake Table Blind Prediction Tests: Contributions for Improved Fiber-based Frame Modelling. Journal of Earthquake Engineering 24:1435–1476. https://doi.org/10.1080/13632469.2018.1466743